SLAC-PUB-9619
January 2003

Perturbation Expansion for High-Gain Free-Electron Laser Saturation*

S. Krinsky[1]
Stanford Linear Accelerator Center, Stanford, CA 94309

Abstract

We develop a perturbation expansion for the solution of the nonlinear one-dimensional free-electron laser equations. For a monochromatic wave, the radiation field is expanded in a Taylor series having a finite radius of convergence. Analytic continuation using Pade′ approximates yields accurate results well into the saturation regime. We also formulate the perturbation expansion for finite bandwidth, self-amplified spontaneous-emission (SASE), and determine the lowest order correction to the well-known linear theory. Motivated by an approximation to the expansion coefficients, we introduce a simplified model for the SASE radiation field, and use it to discuss SASE statistics in the saturation regime, before the onset of the sideband instability.

Submitted to: Physical Review ST-AB

[1] Permanent address: Brookhaven National Laboratory, Upton, NY 11973

* Work supported by Department of Energy contracts DE–AC03–76SF00515 and DE-AC02-98CH10886.

I. INTRODUCTION

Free-Electron Laser (FEL) amplifiers in the exponential growth regime are accurately described by linear equations, which have been studied in great detail [1-13] and are very well understood. The theory of FELs in this linear region of operation is quite mature. On the other hand, the theoretical description [14-19] of the saturation of the gain process due to nonlinear phenomena is in a less advanced state. At present, most studies of saturation are based upon computer simulation [20-22].

In this paper, we develop a perturbation expansion to treat the nonlinearity in the one-dimensional free-electron laser equations. For a monochromatic wave, the resulting Taylor series for the radiation field has a finite radius of convergence. We find that analytic continuation using Pade′ approximates yields results in agreement with numerical integration of the equations, well into saturation.

We also formulate the perturbation expansion for finite bandwidth, self-amplified spontaneous-emission (SASE). Motivated by the narrowness of the FEL gain-bandwidth, we consider an approximate expression for the nonlinear SASE radiation field, in terms of the result of linear SASE theory and the solution of the nonlinear single-frequency FEL equations. This simplified model for the nonlinear SASE field is used to obtain an approximate description of the statistical properties of SASE in the saturation regime. We obtain good agreement with the simulation results of ref. [22] before the onset of the sideband instability.

The perturbation expansion is developed in Section II for the case of amplification of a monochromatic wave, and in Section III, for finite bandwidth SASE. Motivated by an approximation to the expansion coefficients, we suggest in Section IV a simplified model for the nonlinear SASE field and use this model in Section V to obtain an approximate description of the statistical properties of SASE in the saturation regime. A summary of results is given in Section VI.

II. SINGLE FREQUENCY

The scaled equations [4] for the evolution of a one-dimensional electron distribution and a monochromatic radiation field are:

$$\frac{d\theta_j}{dZ} = p_j , \tag{2.1}$$

$$\frac{dp_j}{dZ} = -Ae^{i\theta_j} - A^* e^{-i\theta_j} , \tag{2.2}$$

$$\frac{dA}{dZ} = \left\langle e^{-i\theta_j} \right\rangle . \tag{2.3}$$

$\theta_j = (k_s + k_w)z - \omega_s t_j(z)$ is the phase of the jth electron relative to the radiation and and $p_j = (\gamma - \gamma_0)/\rho\gamma_0$ is its (scaled) energy deviation. We define : γ the relativistic parameter; $Z = 2\rho k_w z$ the scaled distance along the undulator axis; $2\pi/k_w$ the undulator period; $2\pi/k_s$ the radiation wavelength; and $t_j(z)$ the arrival time of the jth electron at position z. The radiated electric field has the form $E\exp[ik_s(z-ct)]$ and the scaled amplitude $A \equiv E/\sqrt{\rho n_0 \gamma_0 mc^2/\varepsilon_0}$ (mks units), where ρ is the Pierce parameter and n_0 the electron density. The bracket $\langle\ \rangle$ indicates the average over the initial electron distribution. The average energy loss per electron is given by

$$\left\langle \Delta\gamma/\gamma_0 \right\rangle = -\rho|A|^2 , \tag{2.4}$$

and the average radiated power per unit area is

$$P/\Sigma = (n_0 c)(\gamma_0 mc^2)\left\langle -\Delta\gamma/\gamma_0 \right\rangle , \tag{2.5}$$

equal to the electron flux, $n_0 c$, times the average energy loss per electron.

We shall develop the solution of Eqs. (2.1-2.3) as a perturbation expansion in the small parameter ε , which we take to be the initial value of the radiation amplitude,

$$A(0) = \varepsilon . \tag{2.6}$$

Without loss of generality we can consider ε to be real. Expanding in powers of ε , we write:

$$\theta(Z) = \theta_0 + p_0 Z + \varepsilon\theta_1(Z,\theta_0,p_0) + \varepsilon^2\theta_2(Z,\theta_0,p_0) + \cdots , \tag{2.7}$$

$$A(Z) = \varepsilon A_1(Z) + \varepsilon^3 A_3(Z) + \varepsilon^5 A_5(Z) + \cdots . \tag{2.8}$$

The constraints:

$$\theta_n(0) = \theta_n'(0) = 0, \qquad (n \geq 1) \tag{2.9}$$

$$A_1(0) = 1, \quad A_n(0) = 0, \quad (n \geq 3) \tag{2.10}$$

assure that $\theta(0) = \theta_0$, $\theta'(0) = p_0$, and $A(0) = \varepsilon$. For an initially uniform electron beam, and a monochromatic electromagnetic wave, the system is periodic so we can restrict our attention to the interval $0 \leq \theta_0 \leq 2\pi$.

The electron beam entering the undulator at $Z = 0$ is described by the distribution $f(\theta_0, p_0)$. The average of a quantity $O(\theta_0, p_0)$ is defined to be

$$\langle O \rangle \equiv \int d\theta_0 dp_0 O(\theta_0, p_0) f(\theta_0, p_0). \tag{2.11}$$

If the electron beam is initially monoenergetic with zero detuning $(p_0 = 0)$, the distribution is

$$f(\theta_0, p_0) = \frac{1}{2\pi} \delta(p_0). \tag{2.12}$$

In this case,

$$\langle \cdots \rangle \equiv \int \frac{d\theta_0}{2\pi} \cdots, \tag{2.13}$$

and

$$\left\langle e^{-im\theta_0} \right\rangle = \delta_{m,0}, \tag{2.14}$$

where $\delta_{m,0}$ is the Kronecker delta which equals unity for $m = 0$ and vanishes for all $m \neq 0$.

Eqs. (2.1)-(2.3) imply:

$$\theta'' = -Ae^{i\theta} - A^* e^{-i\theta}, \tag{2.15}$$

$$A''' - iA = iA^* \left\langle e^{-2i\theta} \right\rangle - \left\langle \theta'^2 e^{-i\theta} \right\rangle. \tag{2.16}$$

The prime denotes derivative with respect to Z. Let us insert the expansions of Eqs. (2.7) and (2.8) into Eqs. (2.15) and (2.16), and equate terms having equal powers of ε. In this manner we find:

$$\theta_1'' = -A_1 e^{i\theta_0} - A_1^* e^{-i\theta_0}, \tag{2.17}$$

$$\theta_2'' = -iA_1\theta_1 e^{i\theta_0} + iA_1^* \theta_1 e^{-i\theta_0}, \tag{2.18}$$

$$A_1''' - iA_1 = 0, \tag{2.19}$$

$$0 = iA_1^* \left\langle e^{-2i\theta_0}(-2i\theta_1)\right\rangle - \left\langle \theta_1'^2\, e^{-i\theta_0}\right\rangle, \tag{2.20}$$

$$A_3''' - iA_3 = iA_1^* \left\langle e^{-2i\theta_0}(-2i\theta_2 - 2\theta_1^2)\right\rangle - \left\langle e^{-i\theta_0}(-i\theta_1'^2\,\theta_1 + 2\theta_1'\theta_2')\right\rangle. \tag{2.21}$$

The first-order amplitude A_1 has the well-known solution [1,3,4],

$$A_1(Z) = \frac{1}{3}\left(e^{sZ} + e^{-s^*Z} + e^{-iZ}\right) \tag{2.22}$$

where

$$s = \frac{\sqrt{3}}{2} + \frac{i}{2}. \tag{2.23}$$

There are three modes: growing; decaying and oscillating. For $Z >> 1$, the exponentially growing mode dominates and

$$A_1(Z) \cong \frac{1}{3} e^{sZ}. \tag{2.24}$$

Since we are interested in the leading behavior for large Z, we can use the approximation (2.24). We then find from Eqs. (2.17) and (2.18) that

$$\theta_1 \cong -\frac{1}{s^2} A_1 e^{i\theta_0} - \frac{1}{s^{*2}} A_1^* e^{-i\theta_0}, \tag{2.25}$$

$$\theta_2 \cong \frac{1}{4s} A_1^2 e^{2i\theta_0} - \frac{1}{s+s^*} A_1 A_1^* + \frac{1}{4s^*} A_1^{*2}\, e^{-2i\theta_0}. \tag{2.26}$$

We have dropped terms that are needed to satisfy the initial conditions of Eqs. (2.9) and (2.10), but are negligible for large Z. Inserting Eqs. (2.25) and (2.26) into Eq. (2.21), we derive

$$A_3''' - iA_3 = \left(-\frac{9\sqrt{3}}{4} + \frac{i}{4}\right) A_1^2 A_1^*. \tag{2.27}$$

Since the right-hand side of Eq. (2.27) has a simple exponential Z-dependence, $\exp[(2s + s^*)Z]$, the inhomogeneous solution is easily found. The homogeneous solution is required to satisfy the initial condition of Eq. (2. 10), but is negligible for large Z. For this reason, we keep only the inhomogeneous solution and write

$$A_3 \cong \left(\frac{-13 + i5\sqrt{3}}{72} \right) A_1^2 A_1 * . \tag{2.28}$$

Extending the approach outlined above one can show that for large Z, the perturbation coefficients θ_n and A_n have the form:

$$\theta_n(Z, \theta_0) = \sum_{k=0}^{n} b(n, n-2k) A_1^{n-k}(Z) A_1 *^k (Z) e^{i(n-2k)\theta_0} , \quad (n \geq 1) \tag{2.29}$$

and

$$A_{2m+1}(Z) = a(m) A_1^{m+1}(Z) A_1 *^m (Z) . \qquad (m \geq 0) \tag{2.30}$$

$b(n, n-2k)$ and $a(m)$ are complex constants independent of Z, to be determined recursively from Eqs. (2.15) and (2.16). $a(0) = 1$. We have already found θ_1, θ_2 and A_3 as given in Eqs. (2.25), (2.26) and (2.28). Next, we can determine θ_3, θ_4 from Eq. (2.15). Once this is accomplished, A_5 can be found from Eq. (2.16). In general, suppose we know $\theta_1, \theta_2, \cdots, \theta_{2m}$ and $A_1, A_3, \cdots, A_{2m+1}$, then θ_{2m+1} and θ_{2m+2} can be determined from Eq. (2.15), and then A_{2m+3} can be found from Eq. (2.16).

Let us introduce the new variable,

$$\xi \equiv \frac{1}{9} \varepsilon^2 e^{\sqrt{3} Z} . \tag{2.31}$$

From Eqs. (2.8) and (2.30), we see that the radiation amplitude satisfies the scaling relation:

$$A(Z; \varepsilon) e^{-iZ/2} \cong \sqrt{\xi}\, h(\xi) , \qquad (Z >> 1) \tag{2.32}$$

with

$$h(\xi) = \sum_{m=0}^{\infty} a(m) \xi^m . \tag{2.33}$$

The fact that the right-hand side of Eq. (2.32) does not depend on ε and Z independently, but only in the combination specified in Eq. (2.31), means that for large Z a change in the initial value of the radiation field, ε, corresponds to a translation in Z.

Using Mathematica we have computed the coefficients a(1),…,a(12) of the power series in Eq. (2.33). In Table 1, columns 2 and 3, we present the magnitude and argument

of the complex ratios, $a(n)/a(n-1)$. We see that after the first few values of n, the argument of this ratio remains close to 2.397 rad. The magnitude of the ratio also varies slowly. The variation is further reduced if we multiply by $n/(n-1/2)$. These results

n	$\lvert a(n)/a(n-1)\rvert$	$Arg[a(n)/a(n-1)]$	$\lvert a(n)/a(n-1)\rvert\frac{n}{n-1/2}$
1	.216951	2.55393	.433903
2	.272966	2.43870	.363955
3	.298157	2.42034	.357788
4	.310309	2.40888	.354639
5	.318838	2.40122	.354264
6	.325133	2.39864	.354690
7	.329361	2.39838	.354696
8	.332254	2.39793	.354404
9	.334581	2.39709	.354262
10	.336581	2.39662	.354296
11	.338190	2.39659	.354294
12	.339444	2.39654	.354203

Table 1. Ratios of coefficients in expansion for $h(\xi)$ [Eq. (2.33)]

suggest the existence of an inverse square root branch point at

$$\xi_0 \cong \frac{e^{-i2.397}}{.354}. \tag{2.34}$$

Support for this is given by noting the relation

$$\frac{1}{\sqrt{1-\xi/\xi_0}} = \sum_{n=1}^{\infty} \frac{\Gamma(n+1/2)}{\Gamma(n+1)\Gamma(1/2)}(\xi/\xi_0)^n. \tag{2.35}$$

The singularity limits the radius of convergence of the power series in Eq. (2.33). Therefore in order to use it to study the saturation of the FEL, we need to carry out an analytic continuation. One approach to the analytic continuation of a Taylor series is the use of Pade′ approximates [23]. In this approach, one constructs a sequence of rational functions to approximate the unknown function. The rational functions are chosen such that when they are expanded, the coefficients match the original series expansion as well as possible. As an example [23], let us consider the function

$$f(x)=\left(\frac{1+2x}{1+x}\right)^{1/2}=1+\frac{1}{2}x-\frac{5}{8}x^2+\frac{13}{16}x^3-\frac{141}{128}x^4+\cdots \tag{2.36}$$

Clearly, the Taylor series fails to converge for any value of x>1/2. The first Pade′ approximate is

$$\frac{1+(7/4)x}{1+(5/4)x}=1+\frac{1}{2}x-\frac{5}{8}x^2+\frac{25}{32}x^3-\frac{125}{128}x^4+\cdots . \tag{2.37}$$

This simple approximation has the value 1.4 at $x=\infty$ which should be compared to the exact value, $\sqrt{2}$. The next approximation is

$$\frac{1+(13/4)x+(41/16)x^2}{1+(11/4)x+(29/16)x^2}, \tag{2.38}$$

whose value is 1.4138 at $x=\infty$.

For $Z>>1$, the radiation intensity has the form:

$$\left|A(Z)\right|^2\cong\xi\left|\sum_{m=0}^{\infty}a(m)\xi^m\right|^2\equiv I(\xi). \tag{2.39}$$

In Eq. (2.39), the coefficients a(m) are complex and the variable ξ introduced in Eq. (2.31) is real. We expand the right-hand side of (2.39) in powers of ξ and attempt to analytically continue by using Pade′ approximates. We denote by [M,N], the Pade′ approximate in which the numerator is a polynomial of degree M and the denominator is a polynomial of degree N. In Fig. 1, we plot the intensity $\left|A(Z)\right|^2$ versus Z for the [N,N] approximates, with N=1,…,6. It is seen that convergence out to about $Z=10$ has been achieved for the [5,5] and [6,6] approximates. In Fig. 2, we compare our result to that obtained by numerically integrating Eqs. (2.1)-(2.3). The equations were solved

numerically using Mathematica, taking $A(0) = \varepsilon = .003$, and 1000 electrons, initially equally spaced in phase in the interval $0 \le \theta_j \le 2\pi$. Excellent agreement is observed in the region of convergence of the Pade′ approximates.

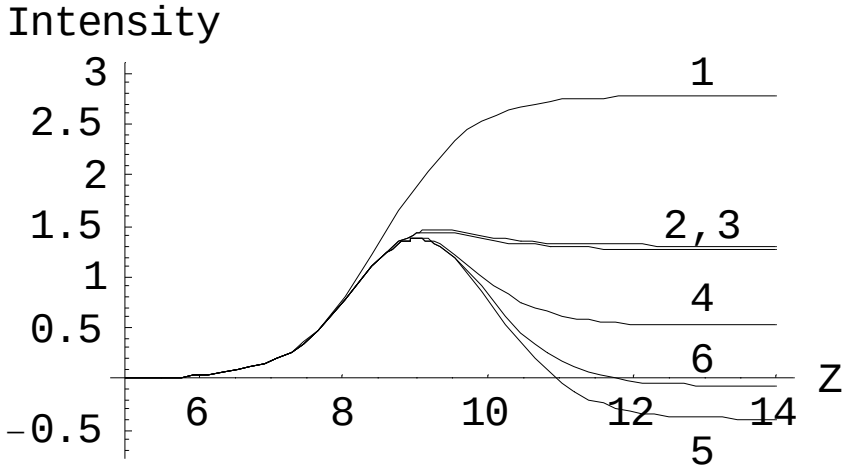

Fig. 1. The dimensionless intensity $|A(Z)|^2$ as derived from the [N,N] (N=1,…,6) Pade′ approximates (for $\varepsilon = .003$) versus dimensionless distance Z traveled along the undulator.

Using Eqs. (2.32) and (2.33), we have calculated a power series expansion for the phase ψ of the radiation field ($A = |A|e^{i\psi}$). In Fig. 3, we compare $\psi - Z/2$ as calculated from the [6,6] Pade′ approximate with the result obtained by numerically integrating Eqs. (2.1)-(2.3). Excellent agreement is observed out to about $Z = 10$.

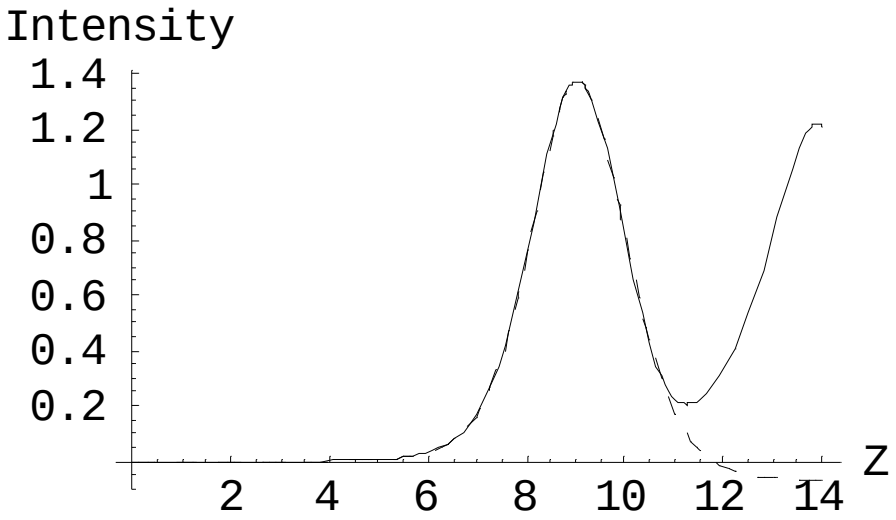

Fig. 2. The dimensionless intensity $|A(Z)|^2$ computed (for $\varepsilon = .003$) from the [6,6] Pade′ approximate (dashed curve), and the result of numerically integrating the 1-D FEL equations (solid curve), plotted versus dimensionless distance Z traveled along the undulator. The agreement is seen to be excellent out to about $Z = 11$.

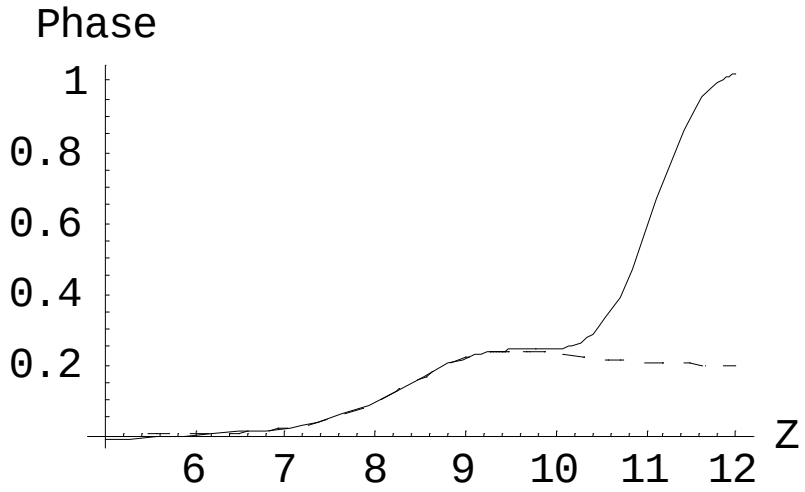

Fig. 3. The radiation phase $\psi - Z/2$ as calculated (for $\varepsilon = .003$) by the [6,6] Pade′ approximate (dashed curve), and by numerically integrating the 1-D FEL equations (solid curve), plotted versus the dimensionless distance Z traveled along the undulator.

It is of interest to compare the result of our analysis with the phenomenological approximation considered by Dattoli and Ottaviani [19]. They suggest modeling the intensity at saturation using the approximate form:

$$P(Z) = \frac{\frac{1}{9} P_0 e^{\sqrt{3}Z}}{1 + \frac{P_0}{9P_{sat}}\left(e^{\sqrt{3}Z} - 1\right)}. \tag{2.40}$$

In our notation, the initial power $P_0 = \varepsilon^2$ and the saturated power P_{sat}=1.4. Hence, their model corresponds to approximating the scaling function $I(\xi)$ [Eq. (2.39)] by

$$I(\xi) \cong \frac{\xi}{1 + \frac{\xi}{1.4}}. \tag{2.41}$$

In Fig. 4, we compare (for $\varepsilon = .003$) the approximation of Eq. (2.41) with the result of numerically solving Eqs. (2.1)-(2.3). It should be noted that the approximation given in Eq. (2.41) is not the [1,1] Pade′ approximate, which was shown in Fig. 1.

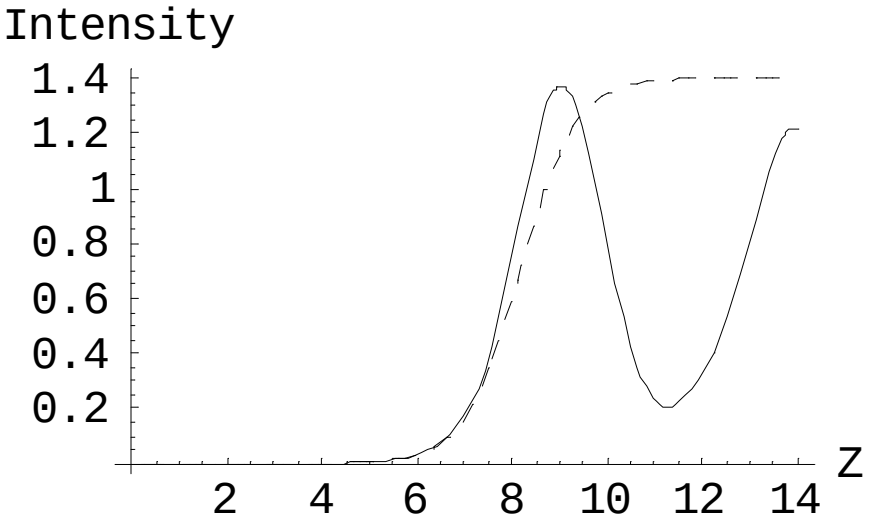

Fig. 4. The dimensionless intensity $|A(Z)|^2$ as computed by numerically solving Eqs. (2.1)-(2.3), solid curve; and as approximated by Eq. (2.41), dashed curve, plotted versus the dimensionless distance Z traveled along the undulator.

III. FINITE BANDWIDTH

We again use the variable $Z = 2\rho k_w z$ as the scaled distance along the undulator axis and introduce the variable $\tau = 2\rho[(k_s + k_w)z - \omega_s t]$ to describe the scaled time along the electron bunch. The phase of the j th electron relative to the radiation is $\theta_j = (k_s + k_w)z - \omega_s t_j(z)$, where $t_j(z)$ is its arrival time at position z. For a coasting electron beam with average electron line density n_1, the one-dimensional FEL equations in time-domain can be written in the form:

$$\frac{d\theta_j}{dZ} = p_j, \tag{3.1}$$

$$\frac{dp_j}{dZ} = -A(Z,2\rho\theta_j)e^{i\theta_j} - A^*(Z,2\rho\theta_j)e^{-i\theta_j}, \tag{3.2}$$

$$\left(\frac{\partial}{\partial Z} + \frac{\partial}{\partial \tau}\right)A = \frac{1}{N_c}\sum_j e^{-i\theta_j}\delta(\tau - 2\rho\theta_j), \tag{3.3}$$

where $N_c = n_1 / 2\rho k_s$ is the number of electrons in a cooperation length $\ell_c = \lambda_s / 4\pi\rho$. These equations are equivalent to those considered in refs. [24,25]. Introducing the Fourier transform,

$$A(Z,\tau) = \int \frac{dq}{2\pi} A_q(Z)e^{iq\tau}, \tag{3.4}$$

we obtain the FEL equations in frequency domain:

$$\frac{d\theta_j}{dZ} = p_j, \tag{3.5}$$

$$\frac{dp_j}{dZ} = -\int \frac{dq}{2\pi}\left[A_q e^{i(1+\hat{q})\theta_j} + A_q^* e^{-i(1+\hat{q})\theta_j}\right], \tag{3.6}$$

$$\frac{dA_q}{dZ} + iqA_q = \frac{1}{N_c}\sum_j e^{-i(1+\hat{q})\theta_j} \equiv \left\langle e^{-i(1+\hat{q})\theta_j}\right\rangle, \tag{3.7}$$

where $\hat{q} \equiv 2\rho q = \dfrac{\Delta\omega}{\omega}$. These equations are equivalent to those considered in refs. [7,26].

As in the single frequency case, we shall look for a solution using a perturbation expansion:

$$\theta(Z) = \theta_0 + \varepsilon\theta_1(Z) + \varepsilon^2\theta_2(Z) + \cdots , \tag{3.8}$$

$$A_q(Z) = \varepsilon A_{1q}(Z) + \varepsilon^3 A_{3q}(Z) + \cdots . \tag{3.9}$$

For finite bandwidth radiation, the system is no longer periodic in θ_0 and for a coasting electron beam we must consider the interval $-\infty < \theta_0 < \infty$. The average behavior of the coasting beam is represented by

$$\left\langle e^{-i\hat{q}\theta_0} \right\rangle = 2\pi\delta(q) . \tag{3.10}$$

Eqs. (3.5-3.7) imply:

$$\theta'' = -\int \frac{dk}{2\pi}\left[A_k e^{i(1+\hat{k})\theta} + A_k * e^{-i(1+\hat{k})\theta} \right], \tag{3.11}$$

$$A_q''' + iqA_q'' - iA_q = i\int \frac{dk}{2\pi} A_k * \left\langle e^{-i(2+\hat{k}+\hat{q})\theta} \right\rangle - \left\langle \theta'^2\, e^{-i(1+\hat{q})\theta} \right\rangle . \tag{3.12}$$

Inserting the expansions of Eqs. (3.8) and (3.9) into Eqs. (3.11) and (3.12), and equating terms having equal powers of ε, we find:

$$\theta_1'' = -\int \frac{dk}{2\pi}\left[A_{1k} e^{i(1+\hat{k})\theta_0} + A_{1k} * e^{-i(1+\hat{k})\theta_0} \right], \tag{3.13}$$

$$\theta_2'' = \int \frac{dk}{2\pi}\left[-iA_{1k}\theta_1 e^{i(1+\hat{k})\theta_0} + iA_{1k} * \theta_1 e^{-i(1+\hat{k})\theta_0} \right], \tag{3.14}$$

$$A_{1q}''' + iqA_{1q}'' - iA_{1q} = 0 , \tag{3.15}$$

$$0 = i\int \frac{dk}{2\pi} A_{1k} * \left\langle e^{-i(2+\hat{k}+\hat{q})\theta_0}\left(-2i\theta_1\right) \right\rangle - \left\langle \theta_1'^2\, e^{-i(1+\hat{q})\theta_0} \right\rangle , \tag{3.16}$$

$$A_{3q}''' + iqA_{3q}'' - iA_{3q} = i\int \frac{dk}{2\pi} A_{1k} * \left\langle e^{-i(2+\hat{k}+\hat{q})\theta_0}\left(-2i\theta_2 - 2\theta_1^2\right) \right\rangle - \left\langle e^{-i(1+\hat{q})\theta_0}\left(-i\theta_1'^2\,\theta_1 + 2\theta_1'\theta_2'\right) \right\rangle \tag{3.17}$$

In the case of SASE, the first-order amplitude has the well-known solution:

$$A_{1q}(Z) = \Lambda_q \left[\frac{s_a e^{s_a Z}}{(s_a - s_b)(s_a - s_c)} + \frac{s_b e^{s_b Z}}{(s_b - s_c)(s_b - s_a)} + \frac{s_c e^{s_c Z}}{(s_c - s_a)(s_c - s_b)} \right] \equiv \Lambda_q G(Z, q) , \tag{3.18}$$

where the shot noise in the beam is represented by

$$\varepsilon \Lambda_q = \frac{1}{N_c} \sum_j e^{-i(1+\hat{q})\theta_j(0)} . \tag{3.19}$$

In the discussion leading to Eq. (5.4) in Section V, we note that a reasonable choice for the perturbation parameter is $\varepsilon = 1/\sqrt{N_c}$. In Eq. (3.18), s_a, s_b, s_c are the three solutions of the cubic equation,

$$s^3 - iqs^2 - i = 0 . \tag{3.20}$$

A useful approximation is

$$s \cong \mu - \frac{i}{3} q - \frac{1}{9\mu} q^2 . \tag{3.21}$$

The three modes: growing; decaying and oscillating; correspond to $\mu = \frac{\sqrt{3}}{2} + \frac{i}{2}, \ -\frac{\sqrt{3}}{2} + \frac{i}{2}, \ -i.$ For $Z >> 1$, the exponentially growing mode dominates and

$$A_{1q}(Z) = G(Z, q)\Lambda_q \cong C_q e^{s_q Z} , \tag{3.22}$$

where we denote the exponent of the growing mode by s_q . Its real part is approximated by

$$\text{Re } s_q \cong \frac{\sqrt{3}}{2} \left[1 - \frac{1}{9} q^2 \right], \tag{3.23}$$

and

$$\left| G(Z, q) \right|^2 \cong \frac{1}{9} \exp\left(\sqrt{3}\, Z \right) \exp\left(-\frac{1}{9} \sqrt{3}\, Z q^2 \right). \tag{3.24}$$

Let us now determine the first nonlinear correction to the SASE field amplitude. From Eqs. (3.13) and (3.14), we find

$$\theta_1 = -\int \frac{d\ell}{2\pi}\left[\frac{A_{1\ell}}{s_\ell^{\,2}} e^{i(1+\hat{\ell})\theta_0} + \frac{A_{1\ell}{}^*}{s_\ell{}^{*2}} e^{-i(1+\hat{\ell})\theta_0}\right] \tag{3.25}$$

$$\theta_2 = i\int \frac{dp}{2\pi}\frac{d\ell}{2\pi}\left[\begin{array}{l} \dfrac{A_{1p}A_{1\ell}}{s_\ell^2(s_p+s_\ell)^2} e^{i(2+\hat{p}+\hat{\ell})\theta_0} + \dfrac{A_{1p}A_{1\ell}{}^*}{s_\ell{}^{*2}(s_p+s_\ell{}^*)^2} e^{i(\hat{p}-\hat{\ell})\theta_0} \\ -\dfrac{A_{1p}{}^*A_{1\ell}}{s_\ell^2(s_p{}^*+s_\ell)^2} e^{-i(\hat{p}-\hat{\ell})\theta_0} - \dfrac{A_{1p}{}^*A_{1\ell}{}^*}{s_\ell{}^{*2}(s_p{}^*+s_\ell{}^*)^2} e^{-i(2+\hat{p}+\hat{q})\theta_0} \end{array}\right]. \tag{3.26}$$

Using these results in Eq. (3.17) leads to the equation,

$$A_{3q}'''+iqA_{3q}''-iA_{3q} = i\int \frac{dk}{2\pi}\frac{dp}{2\pi}\frac{d\ell}{2\pi} f_3(k,p,\ell)A_{1k}A_{1p}A_{1\ell}{}^* 2\pi\delta(p+k-\ell-q), \tag{3.27}$$

where we have defined

$$\begin{aligned} f_3(k,p,\ell) \equiv{}& \frac{2}{s_k^2}\left[\frac{1}{(s_p+s_k)^2} - \frac{1}{s_p^2}\right] \\ &-\left[\frac{2}{s_k^2 s_p s_\ell{}^*} + \frac{1}{s_\ell{}^{*2} s_p s_k} - \frac{2}{s_k s_\ell{}^{*2}(s_p+s_\ell{}^*)} + \frac{2}{s_k s_p^2(s_p+s_\ell{}^*)} - \frac{2}{s_\ell{}^* s_k^2(s_p+s_k)}\right] \end{aligned} \tag{3.28}$$

Using Eq. (3.22), the inhomogeneous solution of Eq. (3.27) is found to be

$$A_{3q}(Z) = i\int \frac{dk}{2\pi}\frac{dp}{2\pi}\frac{d\ell}{2\pi}\frac{f_3(k,p,\ell)A_{1k}(Z)A_{1p}(Z)A_{1\ell}{}^*(Z)2\pi\delta(p+k-\ell-q)}{(s_k+s_p+s_\ell{}^*)^3 + iq(s_k+s_p+s_\ell{}^*)^2 - i}. \tag{3.29}$$

As in the single-frequency case, we do not keep the homogeneous solution that is required to satisfy the initial conditions, because it is negligible for large Z.

IV. SIMPLIFIED MODEL FOR SASE

In the previous section, we developed a systematic perturbation expansion for the case of finite bandwidth SASE, and explicitly found the lowest order correction to the well-known linear theory. Unfortunately, the determination of the higher-order terms appears to be complex. We shall not attempt to compute the higher-order terms in this paper, but shall instead consider a simplified model that is suggested by an approximation to the coefficients in the perturbation series. The motivation for our approximation is the observation that for $Z >> 1$, the first-order solution A_{1k} is sharply peaked about k=0. Therefore, it seems reasonable to consider approximating $s_k \cong s_{k=0} \equiv s$ in the expression for f_3 in Eq. (3.28) and in the denominator of the integrand of Eq. (3.29). We also set q=0 in the denominator. It then follows that

$$A_{3q} \cong \frac{\left(-9\sqrt{3}+i\right)/4}{(2s+s^*)^3 - i} \int \frac{dk}{2\pi}\frac{dp}{2\pi}\frac{d\ell}{2\pi} A_{1k} A_{1p} A_{1\ell} * 2\pi\delta(p+k-\ell-q). \tag{4.1}$$

Noticing that the integral on the right-hand side is the convolution of the Fourier transforms, we can rewrite this expression in terms of the time-domain amplitude. We obtain,

$$A_{3q}(Z) \cong a(1)\int \frac{d\tau}{2\pi} A_1^2(Z,\tau) A_1^*(Z,\tau) e^{-iq\tau}, \tag{4.2}$$

where the coefficients a(m) were defined in Eq. (2.30). The Fourier transform of this result is

$$A_3(Z,\tau) \cong a(1) A_1^2(Z,\tau) A_1^*(Z,\tau), \tag{4.3}$$

In the same spirit, the general term in the perturbation expansion can be approximated by:

$$A_{2m+1}(Z,\tau) \cong a(m)\, A_1^{m+1}(Z,\tau) A_1^{*m}(Z,\tau). \tag{4.4}$$

Note that Eq. (4.4) reduces to Eq. (2.30) when $A_1(Z,\tau)$ is replaced by a function $A_1(Z)$ independent of τ. It then follows from Eqs. (4.4) and (3.9) that for $Z >> 1$,

$$A(Z,\tau;\varepsilon) \cong \varepsilon A_1(Z,\tau) h\left(\varepsilon^2 \left|A_1(Z,\tau)\right|^2\right), \tag{4.5}$$

where,

$$h(\xi) = \sum_{m=0}^{\infty} a(m)\xi^m \tag{4.6}$$

was previously defined in Eq. (2.33) of Section II. Therefore, we have introduced a model in which the SASE radiation field is expressed in terms of the linear approximation $\varepsilon A_1(Z,\tau)$, and the function $h(\xi)$ determined by the solution of the nonlinear single-frequency equations (2.1)-(2.3). Slippage is taken into account in the linear approximation, but not in the function $h(\xi)$ that approximates saturation.

The function $h(\xi)$ can be evaluated from the Pade′ approximate of Section II. It can also be determined by direct numerical integration of the single frequency equations. Let $A_{sf}(Z)$ denote the solution to Eqs. (2.1)-(2.3) corresponding to the initial condition $A_{sf}(0) = \varepsilon_{sf}$, then

$$\sqrt{\xi}h(\xi) = A_{sf}(Z_0(\xi))e^{-iZ_0(\xi)/2}, \tag{4.7}$$

with

$$Z_0(\xi) = (\ell n\xi + \ell n(9/\varepsilon_{sf}^2))/\sqrt{3}. \tag{4.8}$$

The model intensity has the form:

$$\left|A(Z,\tau;\varepsilon)\right|^2 \cong I\left(\varepsilon^2\left|A_1(Z,\tau)\right|^2\right), \tag{4.9}$$

where the function $I(\xi)$ was previously defined in Eq. (2.39) and can be expressed as

$$I(\xi) = \left|A_{sf}(Z_0(\xi))\right|^2. \tag{4.10}$$

Let us discuss the expected region of validity of the approximate expression for the SASE amplitude given in Eq. (4.5). Suppose at position Z along the undulator, early in saturation, the SASE pulse is comprised of temporal spikes [27] having widths equal to a few cooperation lengths ($\lambda_s/4\pi\rho$). The field amplitude at this point is still reasonably described by the linear approximation. As the electrons travel several more gain lengths down the undulator, the slippage is on the order of the coherence length, so the energy transfer between the electrons and field may take place in a manner similar to the steady state case discussed in Section II, and the model of Eq. (4.5) may provide a useful description. But as the electrons continue further along the undulator, the slippage exceeds the original coherence length and the model can be expected to lose validity. Eq. (4.5) cannot explain all of the features observed in computer simulations [22] based upon solution of the time-dependent FEL equations. In the model, the intensity of the spikes saturates at the "steady state" value given by the solution of the single-frequency

equations. Effects due to frequency chirping [28] in the spikes may make it possible for higher saturation values to be reached, and these effects are not included in the model.

V. NONLINEAR SASE STATISTICS

For SASE, in the linear regime, it follows from Eqs. (3.18) and (3.19) that

$$\varepsilon A_{1q}(Z) \cong G(Z,q)\frac{1}{N_c}\sum_j e^{-i(1+\hat{q})\theta_j(0)} \ . \tag{5.1}$$

The start-up from shot noise in the electron beam is described by considering the initial electron phases $\theta_j(0)$ as stochastic variables uniformly distributed [22,29]. Averaging over the stochastic ensemble, one finds:

$$C(Z,\tau_a-\tau_b) \equiv \left\langle \varepsilon A_1(Z,\tau_a)\varepsilon A_1{}^*(Z,\tau_b)\right\rangle = \frac{1}{N_c}\int \frac{dq}{2\pi}\left|G(Z,q)\right|^2 e^{iq(\tau_a-\tau_b)}, \tag{5.2}$$

and

$$\left\langle \left|\varepsilon A_1(Z,\tau_a)\right|^2 \left|\varepsilon A_1(Z,\tau_b)\right|^2 \right\rangle = C^2(Z,0) + \left|C(Z,\tau_a-\tau_b)\right|^2 . \tag{5.3}$$

Eq. (5.2) suggests that a reasonable choice for the perturbation parameter is

$$\varepsilon = 1/\sqrt{N_c} \ . \tag{5.4}$$

In the region of exponential growth, we can use the approximation for $\left|G(Z,q)\right|^2$ given in Eq. (3.24) to derive

$$C(Z,\tau) \cong i_{av}(Z)\exp\left(\frac{-\pi\tau^2}{2\tau_c^2(Z)}\right), \tag{5.5}$$

where the coherence time in the linear regime is given by

$$\tau_c(Z) = \sqrt{\frac{2\pi Z}{3\sqrt{3}}} \ , \tag{5.6}$$

and the average intensity is

$$i_{av}(Z) = \left\langle \left|\varepsilon A_1(Z,\tau)\right|^2 \right\rangle \cong \frac{\exp(\sqrt{3}Z)}{9\sqrt{2}\ N_c\tau_c(Z)} \ . \tag{5.7}$$

Now let us use Eqs. (4.5) and (4.10) to discuss the statistics of SASE in the nonlinear saturation regime [22]. Since the SASE intensity in the linear regime is described by the exponential distribution [22], $\frac{1}{\langle I \rangle}\exp\left(-I/\langle I \rangle\right)$, we can express the average nonlinear SASE intensity in the form:

$$\left\langle \left|A(Z,\tau)\right|^2 \right\rangle = \int dQ \exp(-Q) I(Q\, i_{av}(Z)) . \tag{5.8}$$

We also can write

$$\left\langle \left|A(Z,\tau)\right|^4 \right\rangle = \int dQ \exp(-Q) I^2(Q\, i_{av}(Z)) . \tag{5.9}$$

The intensity fluctuation is then given by

$$\sigma_I^2(Z) = \frac{\left\langle \left|A(Z,\tau)\right|^4 \right\rangle - \left\langle \left|A(Z,\tau)\right|^2 \right\rangle^2}{\left\langle \left|A(Z,\tau)\right|^2 \right\rangle^2} . \tag{5.10}$$

In Fig. 5, we plot the average intensity $\left\langle \left|A(Z,\tau)\right|^2 \right\rangle$ versus Z, as determined from Eq. (5.8). In this figure and those that follow, we have chosen:

$$N_c = n_1 \lambda_s / 4\pi\rho = 1.5\times 10^7 . \tag{5.11}$$

In ref. [22], they define $N_c = n_1 \lambda_s / 2\pi\rho$, so the value given in Eq. (5.11) corresponds to the value of 3×10^7 used in their calculations. Fig. 5 is in good agreement with their Fig. 6.13 out to about Z=14. After this point their simulations are dominated by spectral broadening phenomena not included in our simplified model. In Fig. 6, we plot the intensity fluctuation $\sigma_I(Z)$ as determined from Eq. (5.10). The fluctuation at the intensity maximum at Z=13 is about 25% which is one half of that found in the simulations (Fig. 6.15) of ref. [22].

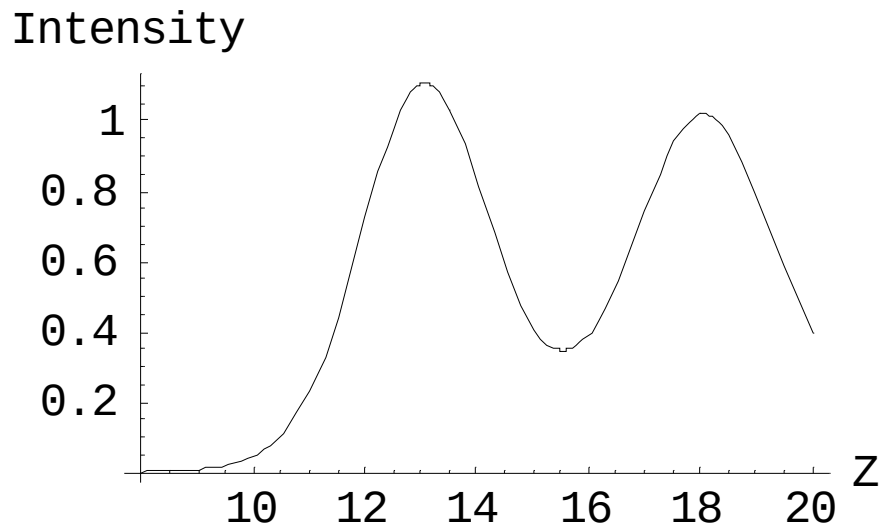

Fig. 5. The average dimensionless SASE intensity calculated from Eq. (5.8), plotted versus the dimensionless distance Z traveled along the undulator.

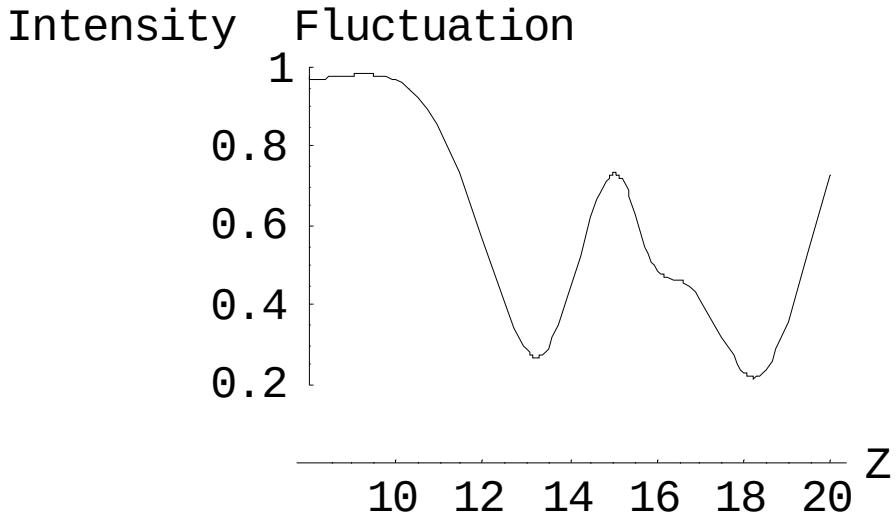

Fig. 6. The SASE intensity fluctuation $\sigma_I(Z)$ as determined from Eq. (5.10), plotted against the dimensionless distance Z traveled along the undulator.

The intensity correlation can be expressed in the form:

$$\left\langle \left|A(Z,\tau_a)\right|^2 \left|A(Z,\tau_b)\right|^2 \right\rangle = \int dQ_a dQ_b P_0(Q_a, Q_b; Z, \tau_a - \tau_b) I(Q_a\ i_{av}(Z)) I(Q_b\ i_{av}(Z)),$$

(5.12)

where the joint probability $P_0(Q_a, Q_b; Z, \tau_a - \tau_b)$ for finding the normalized intensity Q_a at τ_a and Q_b at τ_b is given by Eq. (5.13) with k=0 [29]:

$$P_k(Q_a, Q_b; Z, \tau_a - \tau_b) = \frac{\exp\left(\frac{-Q_a}{1-\beta_{ab}}\right)\exp\left(\frac{-Q_b}{1-\beta_{ab}}\right)}{1-\beta_{ab}} I_k\left(\frac{2\sqrt{\beta_{ab}Q_aQ_b}}{1-\beta_{ab}}\right), \qquad (5.13)$$

where

$$\beta_{ab} = \frac{\left\langle |A_1(Z,\tau_a)|^2 |A_1(Z,\tau_b)|^2 \right\rangle}{\left\langle |A_1(Z,\tau_a)|^2 \right\rangle \left\langle |A_1(Z,\tau_b)|^2 \right\rangle} - 1 \cong \exp\left(\frac{-\pi(\tau_a - \tau_b)^2}{\tau_c^2(Z)}\right),$$

(5.14)

and $I_k(x)$ is the Bessel function of imaginary argument.

The radiation field correlation is given by (see Appendix A):

$$\left\langle A(Z,\tau_a)A^*(Z,\tau_b)\right\rangle = \int dQ_a dQ_b P_1(Q_a, Q_b, Z, \tau_a - \tau_b)\sqrt{Q_a i_{av}(Z) Q_b i_{av}(Z)}\, h(Q_a i_{av}(Z))h^*(Q_b i_{av}(Z)) \qquad (5.15)$$

where P_1 is defined by Eq. (5.13) with k=1. The integrand in Eq. (5.15) is symmetric in Q_a and Q_b, hence the field correlation as given within this approximation is real, whereas the precise result is a complex quantity. In our model the spectral broadening at saturation is symmetric, while in simulations it becomes asymmetric due to the sideband instability. In Fig. 7, we show the field correlation before and during saturation. Our results are seen to agree with Figs. 6.16 and 6.17 of ref. [22] upon noting that our definition of the scaled time τ is twice theirs.

Knowledge of the field correlation, allows us to compute the coherence time [22] from the equation

$$\tau_{coh}(Z) = \int_{-\infty}^{\infty} d\tau \left|g_1(Z,\tau)\right|^2, \qquad (5.16)$$

where $g_1(Z,\tau) = \left\langle A(Z,0)A^*(Z,\tau)\right\rangle / \left\langle |A(Z,0)|^2 \right\rangle$. The coherence time is plotted in Fig. 8. The results are seen to be in good agreement with Fig. 6.22 of ref. [22]-- note our definition of τ_{coh} is twice theirs.

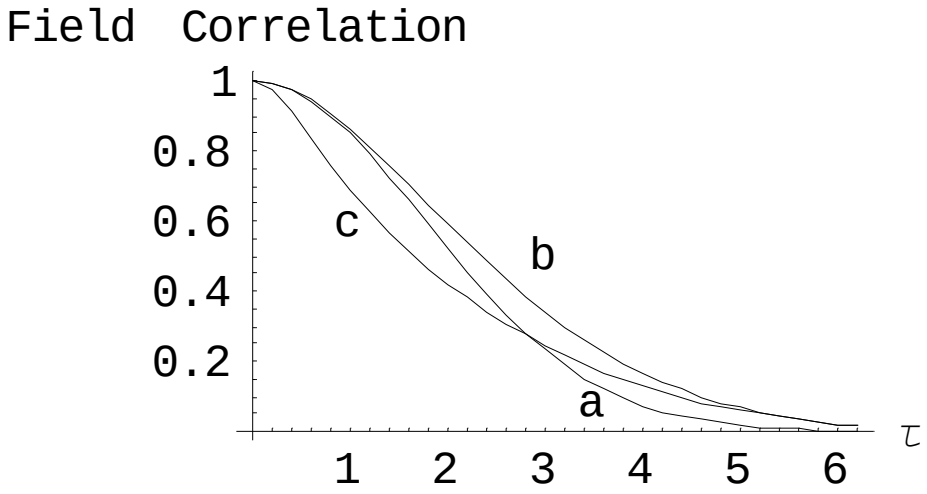

Fig. 7. The field correlation $g_1(Z,\tau) = \langle A(Z,0)A^*(Z,\tau)\rangle / \left\langle |A(Z,0)|^2 \right\rangle$ as given in Eq. (5.15), plotted against dimensionless time τ, for dimensionless distance traveled along the undulator: (a) $Z = 8$; (b) $Z = 13$; and (c) $Z = 15$.

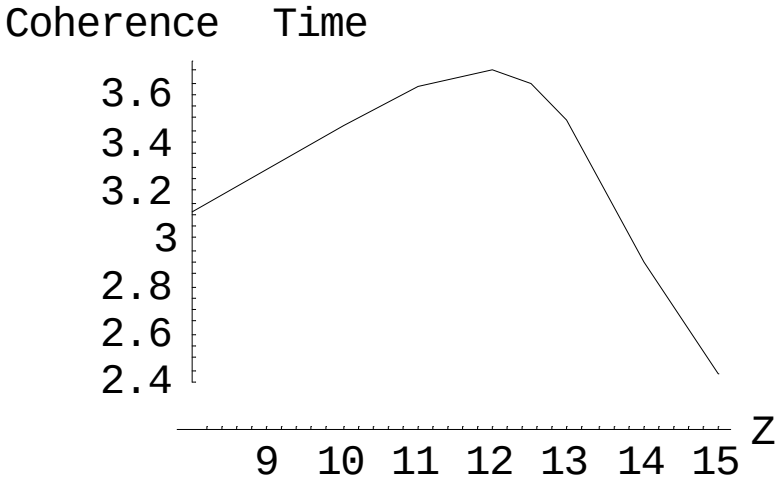

Fig. 9. The dimensionless coherence time $\tau_{coh}(Z)$ as computed from Eq. (5.16) plotted against the dimensionless distance Z traveled along the undulator.

VI. SUMMARY OF RESULTS

In this paper, we develop a perturbation expansion for the solution of the nonlinear one-dimensional FEL equations. In the case of the amplification of a monochromatic input wave (Section II), the perturbation parameter is the initial value of the dimensionless field amplitude, $\varepsilon = A(0) << 1$. For dimensionless distance traveled along the undulator $Z = 2\rho k_w z >> 1$, the amplitude satisfies the scaling relation:

$$A(Z;\varepsilon)\, e^{-iZ/2} \cong \sqrt{\xi}\, h(\xi), \tag{6.1}$$

where the variable ξ is defined by

$$\xi \equiv \frac{1}{9}\varepsilon^2 e^{\sqrt{3}Z}. \tag{6.2}$$

The fact that the right-hand side of Eq. (6.1) does not depend on ε and Z independently, but only in the combination specified in Eq. (6.2), means that for large Z, a change in the initial value of the radiation field, ε, corresponds to a translation in Z. It follows from Eq. (6.1) that the intensity is determined by

$$\left|A(Z;\varepsilon)\right|^2 \cong \xi \left|h(\xi)\right|^2 \equiv I(\xi). \tag{6.3}$$

We have expressed the function $h(\xi)$ in a Taylor series:

$$h(\xi) = \sum_{m=0}^{\infty} a(m)\xi^m, \tag{6.4}$$

having a finite radius of convergence. In order to describe saturation, it is necessary to carry out an analytic continuation. We accomplished this using Pade approximates. Excellent agreement with the numerical solution of the nonlinear single-frequency equations was found well into saturation.

We also studied the perturbation expansion for SASE (Section III). In this case, the perturbation parameter is $\varepsilon = 1/\sqrt{N_c} << 1$, where N_c is the number of electrons in a cooperation length $\ell_c = \lambda_s / 4\pi\rho$. Motivated by the narrow bandwidth of the FEL gain, we approximated the expansion coefficients (Section IV) for $Z >> 1$, obtaining the simplified model for the SASE amplitude,

$$A(Z,\tau;\varepsilon) \cong \varepsilon A_1(Z,\tau)\, h\left(\varepsilon^2 \left|A_1(Z,\tau)\right|^2\right). \tag{6.5}$$

In this equation, $\varepsilon A_1(Z,\tau)$ is the linear approximation to the SASE amplitude at position Z along the undulator, observed at dimensionless time τ in the output pulse. The function $h(\xi)$ is the same as that introduced in Eq. (6.1) for the single-frequency case. Whereas the scaling relation for amplification of a monochromatic wave, Eq. (6.1), is a precise asymptotic relation for large Z, the relation (6.5) for SASE relies on an additional approximation, of limited validity. In particular, the simplified model cannot describe the sideband instability that may occur once saturation has been reached. Slippage is taken into account in the linear approximation $\varepsilon A_1(Z,\tau)$, but not in the function $h(\xi)$ describing saturation.

Some justification for using our model to describe the initial saturation process is as follows: Suppose at position Z along the undulator, early in saturation, the SASE pulse is comprised of temporal spikes [27] having widths equal to a few cooperation lengths ($\lambda_s / 4\pi\rho$). The field amplitude at this point is still reasonably described by the linear approximation. As the electrons travel several more gain lengths down the undulator, the slippage is on the order of the coherence length, so the energy transfer between the electrons and field may take place in a manner similar to the steady state case discussed in Section II, and the model of Eq. (4.5) may provide a useful description. But as the electrons continue further along the undulator, the slippage exceeds the original coherence length and the model can be expected to lose validity. Eq. (4.5) cannot explain all of the features observed in computer simulations [22] based upon solution of the time-dependent FEL equations. In the model, the intensity of the spikes saturates at the "steady state" value given by the solution of the single-frequency equations. Effects due to frequency chirping [28] in the spikes may make it possible for higher saturation values to be reached, and these effects are not included in the model.

Our approximation for the SASE intensity when $Z >> 1$ has the form:

$$\left|A(Z,\tau;\varepsilon)\right|^2 \cong I\left(\varepsilon^2 \left|A_1(Z,\tau)\right|^2\right), \tag{6.6}$$

where $I(\xi)$ was introduced in Eq. (6.3), during the discussion of the single-frequency case. Using Eqs. (6.5) and (6.6), we have approximately determined the statistical

properties of SASE in the initial stage of saturation (Section V) in terms of the known statistical properties of the linear approximation $\varepsilon A_1(Z,\tau)$.

Overall our model gives a reasonable description of the nonlinear SASE statistics early in the saturation regime (out to about Z=14 in the example considered), providing a good approximation to the average intensity and coherence time, but underestimating the intensity fluctuation. Simulations exhibit phenomena characterized by increased fluctuation and asymmetric spectral broadening that are not included in our approximation.

ACKNOWLEDGEMENTS

I wish to thank Dr. R.L Gluckstern for stimulating discussions and collaboration in analyzing the series coefficients presented in Table 1. I have benefited from communications with Prof. G. Dattoli in regard to the phenomenological description of FEL saturation given in ref. [19], that was a stimulus for the work reported here. I wish to thank Dr. Z. Huang for enlightening comments and discussion of results from his time-dependent FEL code. This work was supported by Department of Energy contracts DE–AC03–76SF00515 and DE-AC02-98CH10886.

REFERENCES

[1] N.M. Kroll and W.A. McMullin, Phys. Rev. **A17**, 300 (1978).

[2] W.B. Colson and S.K. Ride, In Physics of Quantum Electronics, Vol. 7 (Addison-Wesley, Reading, MA, 1980), p377.

[3] Debenev, Y.S., Kondratenko, A.M. and Saldin, E.L., Nucl. Instrum. Methods **A193**, 415 (1982).

[4] R. Bonifacio, C. Pellegrini, and L.M. Narducci, Opt. Commun. **50**, 373 (1984).

[5] J.M. Wang and L.H. Yu, Nucl. Instrum. Meth. **A250**, 484 (1986).

[6] K.J. Kim, Nucl. Instrum. Meth. **A250**, 396 (1986).

[7] S. Krinsky, AIP Conf. Proc. **153** , 1015 (1987).

[8] W.B. Colson, J.C. Gallardo, and P.M. Bosco, Phys. Rev. **A34**, 4875 (1986).

[9] G. T. Moore, Nucl. Instrum. Meth, **A239**, 19 (1985).

[10] K.J. Kim, Phys. Rev. Lett. **57**, 1871 (1986).

[11] S. Krinsky and L.H. Yu, Phys. Rev. **35**, 3406 (1987).

[12] L.H. Yu, S. Krinsky, and R.L. Gluckstern, Phys. Rev. Lett. **64**, 3011 (1990).

[13] M. Xie., Nucl. Instrum. Methods **A445**, 59 (2000).

[14] R. Bonifacio, F. Casagrande, and L. De Salvo Souza, Phys. Rev. **A33**, 2836 (1986).

[15] R. Bonifacio, L. De Salvo Souza, P Pierini and N. Piovella, Nucl. Instrum. Meth. **A296**, 358 (1990).

[16] R.L. Gluckstern, S. Krinsky and H. Okamoto, Phys. Rev. **E47**, 4412 (1993).

[17] Z. Huang and K.J. Kim, Nucl. Instrum. Methods, **A483**, 504 (2002).

[18] N.A. Vinokurov, Z. Huang, O.A. Shevenko and K.J. Kim, Nucl. Instrum. Methods **A475**, 74 (2001).

[19] G. Dattoli and P.L. Ottaviani, Opt. Commun. **204**, 283 (2002).

[20] W.M. Fawley, "A User Manual for GINGER and Its Post-Processor XPLOTGIN", LBNL Report-49625 (2002).

[21] S. Rieche, Nucl. Instrum. Methods **A429**, 243 (1999).

[22] E.L. Saldin, E.A. Schneidmiller, M.V. Yurkov, *The Physics of Free Electron Lasers*, Springer-Verlag, Berlin, 2000, Chapter 6.

[23] G.A. Baker, *Essentials of Pade´Approximates*, Academic Press, New York, 1975.

[24] S. Krinsky, Phys. Rev. **E59**, 1171 (1999).

[25] B.W.J. McNeil, G.R.M. Robb, and D.A. Jaroszynski, Opt. Comm. **165**, 65 (1999).

[26] N. Piovella, AIP Conf. Proc. **413,** 205 (1997).

[27] R. Bonifacio, L. De Salvo, P. Pierini, N. Piovella, and C. Pellegrini, Phys. Rev. Lett. **73**, 70 (1994).

[28] R.W. Warren, J.C. Goldstein, and B.E. Newman, Nucl. Instrum. Meth. **A250**, 19 (1986).

[29] S. Krinsky and R.L. Gluckstern, Nucl. Instrum. Meth. **A483**, 57 (2002).

Appendix A: Derivation of Eq. (5.15)

In the linear regime, let us introduce the normalized field amplitude $a_1(Z,\tau) \equiv A_1(Z,\tau) / \sqrt{\left\langle \left| A_1(Z,\tau) \right|^2 \right\rangle}$. The joint probability $p(x_a, y_a, x_b, y_b; Z, \tau_a - \tau_b)$ that the normalized amplitude has the values, $a_1(Z,\tau_a) = x_a + iy_a = \sqrt{Q_a}\, e^{i\phi_a}$ and $a_1(Z,\tau_b) = x_b + iy_b = \sqrt{Q_b}\, e^{i\phi_b}$, at fixed position Z along the undulator, but at different times τ_a, τ_b, is given by [29]:

$$p(x_a, y_a, x_b, y_b; Z, \tau_a - \tau_b) = \frac{1}{\pi^2 (1-\beta_{ab})} \exp\left(\frac{-x_a^2 - y_a^2 - x_b^2 - y_b^2 - 2u_{ab}(x_a x_b + y_a y_b) - 2v_{ab}(x_a y_b - x_b y_a)}{1-\beta_{ab}} \right) \tag{A1}$$

where

$$\left\langle a_1(Z,\tau_a)\, a_1{}^*(Z,\tau_b) \right\rangle = u_{ab} + iv_{ab} = \sqrt{\beta_{ab}}\, e^{i\psi_{ab}} . \tag{A2}$$

Using the approximate expression of Eq. (4.5) for the nonlinear field amplitude,

$$A(Z,\tau) \cong \varepsilon A_1(Z,\tau) h\left(\varepsilon^2 \left| A_1(Z,\tau) \right|^2 \right), \tag{A3}$$

the correlation function can be written in the form

$$\left\langle A(Z,\tau_a) A^*(Z,\tau_b) \right\rangle = \int dx_a dy_a dx_b dy_b\, p(x_a, y_a, x_b, y_b; Z, \tau_a - \tau_b)\, i_{av}(Z) \sqrt{Q_a Q_b}\, e^{i(\phi_a - \phi_b)} h\left(i_{av}(Z) Q_a \right) h^*\left(i_{av}(Z) Q_b \right) \tag{A4}$$

$i_{av}(\tau)$ was defined in Eq. (5.7). We change the integration variables to Q_a, Q_b, ϕ_a, ϕ_b, and carry out the integrations in (A4) over the phase angles to obtain Eq. (5.15):

$$\left\langle A(Z,\tau_a) A^*(Z,\tau_b) \right\rangle = e^{i\psi_{ab}} \int dQ_a dQ_b P_1(Q_a, Q_b; Z, \tau_a - \tau_b) \sqrt{Q_a i_{av}(Z) Q_b i_{av}(Z)}\, h\left(Q_a i_{av}(Z) \right) h^*\left(Q_b i_{av}(Z) \right) \tag{A5}$$

where P_1 was defined in Eq. (5.13). When β_{ab} is approximated by Eq. (5.14), $\psi_{ab} = 0$.